

# Computer Lab

Natalie Gray, Iman Ebrahimi, and Alex Matilainen  
*Faculty of Science: Lund University*  
 (Dated: May 31, 2023)

## I. INTRODUCTION

Quantum mechanics poses many different types of mathematical problems with real-world significance, however, they can be increasingly more difficult to solve analytically. Many systems are defined by allowing an incoming particle to interact with a certain potential barrier or well. These potentials can range from a simple infinite well to more difficult systems such as an inverse hyperbolic cosine potential. In these cases, numerical methods are a necessary and powerful solution. Two simple but important tactics are the shooting method and the bisection method both of which require a simple recursion formula. The purpose of this exercise was to gain exposure to these methods by calculating the bound energy states and the number of nodes for two different potentials, the inverse squared cosh potential and a double well potential conceived by the superposition of two inverse squared cosh potentials.

## II. THEORETICAL BACKGROUND

The time-independent Schrödinger equation used in the following methods is given by,

$$E\phi(x) = \frac{-\hbar^2}{2m} \frac{d^2\phi(x)}{dx^2} + V(x)\phi(x), \quad (1)$$

where  $V(x)$  is defined as,

$$V(x) = -V_0 \frac{1}{\cosh^2(x/a)}. \quad (2)$$

$V_0$  is the depth of the energy well and  $a$  is a constant that determines the well's width. These values can be seen in Figure 1.

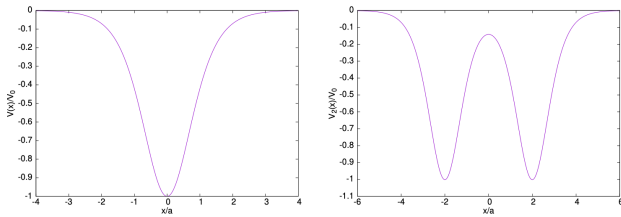


FIG. 1: The figure shows two different plots. The plot on the left is the single potential well and the plot on the right is the double potential well, although both are based on Equation 2. [1].

While this exercise is composed of two different potentials, the second potential is just a slight variation of the first and they are both inverse squared cosh functions. To make the Schrödinger equation easier to manage, it is much simpler to write it in other quantities that are dimensionless. The new equation looks like this,

$$\epsilon\phi(\xi) = -\frac{d^2\phi(\xi)}{d\xi^2} + \nu(\xi)\phi(\xi), \quad (3)$$

where,

$$\nu(\xi) = -\nu_0 \cosh^{-2}(\xi), \quad (4)$$

and the dimensionless substitutions are,

$$\xi = x/a, \epsilon = \frac{2ma^2E}{\hbar^2}, \nu_0 = \frac{2ma^2V_0}{\hbar^2}. \quad (5)$$

The value of  $\nu_0$  is set to a constant value of 6 in the calculations. Simplifying Equation 3 results in a new variable  $f(\xi) = \nu(\xi) - \epsilon$ , which changes the equation to

$$\frac{d^2\phi(\xi)}{d\xi^2} = f(\xi)\phi(\xi). \quad (6)$$

A Taylor expansion to the second order around  $\phi(\xi)$  reveals a necessary recursion formula given by,

$$\phi[i \pm 1] \approx (2 + h^2 f[i])\phi[i] - \phi[i - 1], \quad (7)$$

that allows the calculation of all values of  $\phi$  given knowledge of the first two values of the  $\xi[i]$  mesh, which can be calculated using known boundary conditions [1]. In the equation,  $h$  is the stepsize and  $i$  determines which value on the grid is being pulled. Using the boundary conditions that  $\nu(\xi) \rightarrow 0$  as  $\xi \rightarrow -\infty$ , the B coefficient of the solution to the differential equation in Equation 6 disappears, and what is left is,

$$\phi(\xi) = Ae^{q\xi}, \quad (8)$$

where  $q = \sqrt{-\epsilon}$ . After putting this approximated solution into the center of the potential well, the ratio  $\phi[1]/\phi[0] = e^{qh}$ , which means that  $\phi[0] = 1$  and  $\phi[1] = e^{qh}$ . The recursion formula in Equation 7 and the two previously calculated initial conditions can now be used in the shooting method and bisection method in the code portion of the exercise[1].

### III. METHODS

#### 1) Single-Well Potential Model

##### A) Shooting Method

The impact of varying the energy  $\epsilon$  on the q-value  $\phi[1]$ , the f-function, and the remaining  $\phi[i]$  was observed in order to find eigenvalues using the shooting method. Solutions were sought by adjusting the energy values to obtain a normalized wave function with exponential decay for large positive  $\xi$ . The approach employed was known as the "Shooting Method".

In the implementation of the shooting method, the  $\phi$ -vector was initialized by setting all its elements to zero using the `np.zeros` command. The step-length  $h$  was determined by dividing the difference between  $\xi_{\max}$  and  $\xi_{\min}$  by the number of steps  $N_{\text{steps}}$ . Additionally, the  $\nu(\xi)$ -vector was established, and an initial estimation for the energy value, bounded by  $-\nu_0$  and 0, was made. Further calculations involved defining  $q$ ,  $\phi[0]$ , and  $\phi[1]$  to facilitate the computation of the wave vector  $\phi$  using a for-loop and the recursion relation. The resulting wave function  $\phi$  was visualized by employing the `plt.plot(xi, phi)` command, and the plot was displayed using `plt.show()`.

To validate the code and implemented algorithm, the results were compared with analytically derived solutions for the Schrödinger Equation. For the studied potential, the eigenvalues were determined as  $\epsilon_n = -(b-n)^2$  for all  $n < b$ , where  $\nu_0 = b(b+1)$ . In the specific case of  $\nu_0 = 6$  corresponding to  $b = 2$ , the expected eigenenergies were  $\epsilon_0 = -4$  and  $\epsilon_1 = -1$ , without any additional solutions. The program was executed to investigate the behavior of the wave function for these theoretical eigenenergies. The resulting wave function for the ground state was plotted and subjected to further analysis.

##### B) Bisection Method

In order to automate the process of finding solutions in the single-well potential model, a mathematical criterion that aligns with the visual observation of the function's divergence was employed, known as the bisection method. This method involved examining the behavior of the wave function as  $\xi$  approaches infinity. The computational steps taken were as follows:

Firstly, the target bound state, characterized by the desired number of nodes in the wave function, was determined. An energy range was defined to facilitate the search for solutions. If the minimum energy value yielded an excessive number of nodes or the maximum energy value resulted in an insufficient number of nodes, the search was abandoned, and a notification was printed to indicate that the desired solution could not be found within the specified energy range.

Next, a new energy value was selected as the midpoint between the minimum and maximum energies. To determine whether the energy was too low or too high, two tests were conducted. Firstly, the number of nodes within the range  $[\xi_{\min}, \xi_{\max}]$  was examined. Secondly, the sign of the expression  $\phi[N-1]\phi[N] - e^{qh}\phi[N]^2$  was assessed. A negative value indicated that  $|\phi[N]|$  was excessively large, resulting in a blow-up of the tail with the same sign as  $\phi[N]$ , meaning no new nodes were present. On the other hand, a positive value signified that the slope between  $\phi[N-1]$  and  $\phi[N]$  was too steep, indicating the existence of exactly one additional node beyond  $\xi_{\max}$ .

This process was repeated until the relative energy difference  $(\epsilon_{\min} - \epsilon_{\max})/(\epsilon_{\min} + \epsilon_{\max})$  became smaller than a predefined tolerance of approximately  $10^{-8}$ , corresponding to eight-digit accuracy, or until the precision limit of the computer's floating-point numbers was reached.

The bisection method provides an automated and efficient approach to identifying solutions in the single-well potential model, eliminating the need for manual identification and speeding up the computational process.

#### 2) Double-Well Potential Model

To extend the analysis to the double well potential, the bisection method program implemented in the single-well potential case was modified accordingly. The  $\xi$ -range and parameters were adjusted to handle the double well potential. The computational steps remained similar to Part One, utilizing the modified program to determine bound states and plot energy eigenvalues as a function of the separation parameter  $s$ . Additionally, wave functions for the ground state and first excited state were plotted for large values of  $s$  to gain insights into their behavior.

The computational steps undertaken in the double-well potential case allowed for the analysis of bound states in the double-well potential model, contributing to a comprehensive understanding of the system.

### IV. RESULTS

#### 1) Shooting Method

The number of nodes for both the ground state and first excited state wave functions were found. This was done utilizing the technique discussed more in Sections III and II with the code being presented in the Appendix section at VI. The wave function graphs and  $\epsilon$  values for both the first excited state and ground state were found as well, resulting in Figures 2 and 3 for the ground and first excited states respectively. The answer to all three questions in this section immediately follow the graphs below.

1.1) The ground state wave function has zero nodes, as seen in Figure 2.

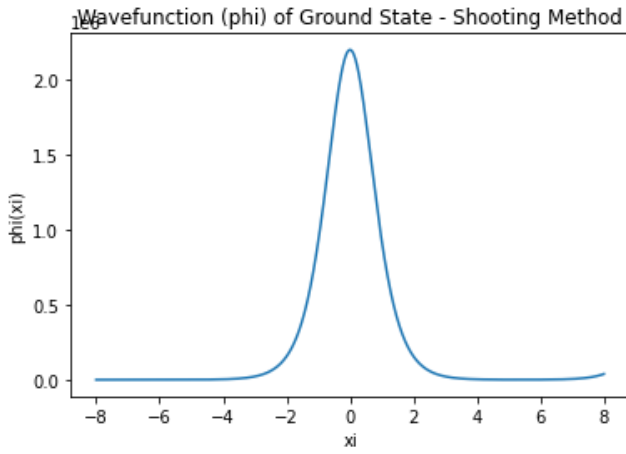


FIG. 2: The figure shows the plot for the wave function of the ground state for the single well potential model with the x-axis being the value of  $\xi$  while the y-axis is  $\phi(\xi)$ . The graph displays the results of running the code in the Appendix in Section VI, which is based on equation (7). The  $\epsilon$  value found for the ground state with the shooting method was  $-3.9990186$ .

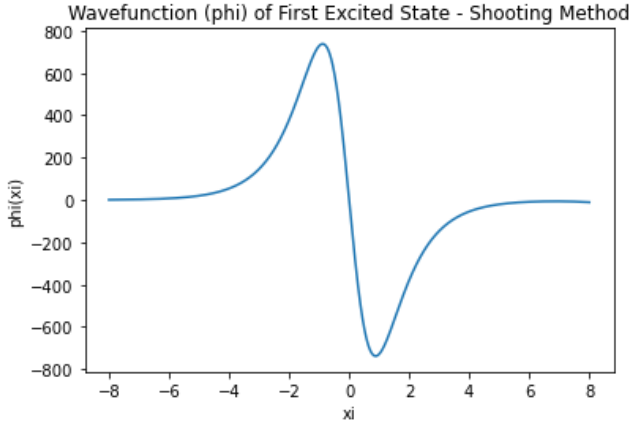


FIG. 3: The figure shows the plot for the wave function of the first excited state of the single well potential model with the x-axis being the value of  $\xi$  while the y-axis is  $\phi(\xi)$ . The graph displays the results of running the code in the Appendix in Section VI, which is based on equation (7). The  $\epsilon$  value found for the first excited state with the shooting method was  $-.9983$ .

1.2) The first excited state wave function has one node, as seen in Figure 3.

1.3) The excited state extends further into space because it has a higher energy eigenvalue when compared to the ground state. This causes the electron to have a greater kinetic energy which increases the likelihood for it to extend further into the further regions of the potential well. This allows the wave function to "penetrate" deeper into the region where the potential energy is lower, whereas the ground

state wave function did not have enough energy to do so causing the wave function to extend further out.

## 2) Bisection Method

For the bisection method section the value for the energy of the ground state and first excited state systems  $\epsilon$  was found utilizing a very similar technique the shooting Method. Where the two methods differ is that the bisection method automates the finding of the  $\epsilon$  value using techniques described more thoroughly in Section III. The wave function graphs and  $\epsilon$  values for both the first excited state and ground state were found as well, resulting in Figures 4 and 5 for the ground and first excited states respectively. The answer to the two questions in this section immediately follow the graphs below.

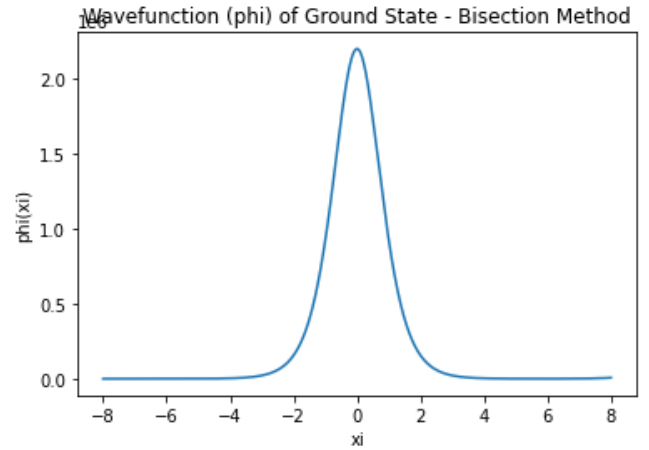


FIG. 4: The figure shows the plot for the wave function of the ground state for the single well potential model with the x-axis being the value of  $\xi$  while the y-axis is  $\phi(\xi)$ . The graph displays the results of running the code in the Appendix in Section VI, which is based on equation (7). The  $\epsilon$  value found for the ground state with the bisection method was  $-3.99902$ .

2.1) The instructions recommend that an upper energy limit of  $\epsilon = 1$  be installed to ensure that the value for the energy  $\epsilon$  never approximately equals zero. This is done because the assumption that " $\nu(\xi \rightarrow -\infty) \approx 0$  is negligible compared to  $\epsilon$ " no longer holds, since  $\epsilon$  is now approximately 0 as well. This results in equation (8) no longer being an accurate approximation of equation (6).

2.2) We unfortunately did not have the time to try large  $\nu_0$  and find the associated eigenenergies.

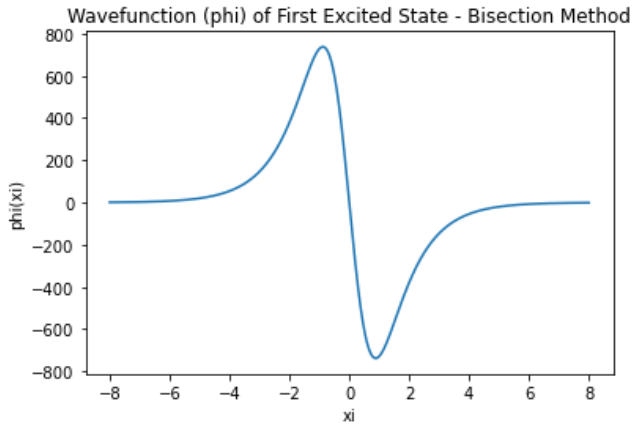


FIG. 5: The figure shows the plot for the wave function of the first excited state of the single well potential model with the x-axis being the value of  $\xi$  while the y-axis is  $\phi(\xi)$ . The graph displays the results of running the code in the Appendix in Section VI, which is based on equation (7). The  $\epsilon$  value found for the first excited state with the bisection method was  $-0.99829$ .

### 3) Double-Well Potential Model

The analysis was expanded onto double well potential models utilizing very similar computational techniques to the shooting and bisection method with updated values for the  $\nu$  parameter and altered ranges for  $\xi$ , as mentioned in Section III. These updates were utilized to determine the relationship between the separation parameter  $s$  and the energy eigenvalues for the various states of the double potential well system, which can be seen in Figure 6. Additionally, the wave functions for the ground and first excited states with large  $s$  ( $s \gg 1$ ) was also found. These two figures can be seen in Figures 7 and 8. The answer to all four questions in this section immediately follow the graphs below.

3.1) For  $s \approx 0$  there were three bound states whereas for  $s \gg 1$  there were two bound states found.

3.2) The energies we obtained for  $s \approx 0$  were somewhat similar to those we obtained from the single well results. We found that for the ground state double well we got a value of  $\epsilon = -8.93037$ , for the first excited state we got  $\epsilon = -3.99659$ , and for the second excited state we got  $\epsilon = -1.01072$ . These values can be seen in Figure 6 as the first data point entered for each one. The first excited is very similar to the value found for the single well potential ground state as seen in Figure 4, while the second excited state is very similar to the single well potential first excited state as seen in Figure 5.

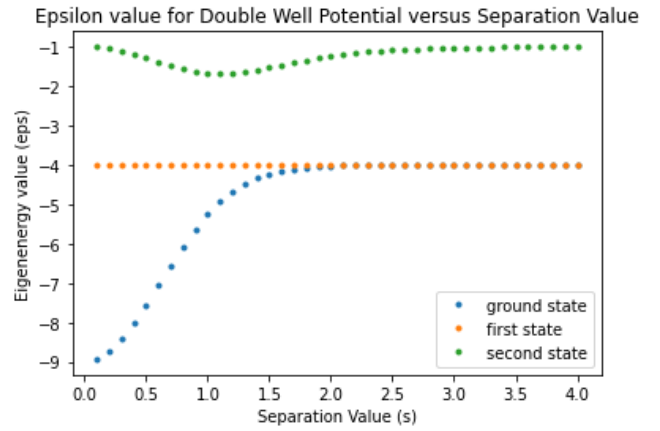


FIG. 6: The figure shows the plot for the wave function of the ground state for the single well potential model with the x-axis being the value of  $\xi$  while the y-axis is  $\phi(\xi)$ . The graph displays the results of running the code in the Appendix in Section VI, which is based on equation (7). The  $\epsilon$  value found for the ground state with the bisection method was  $-3.999018580466508$ .

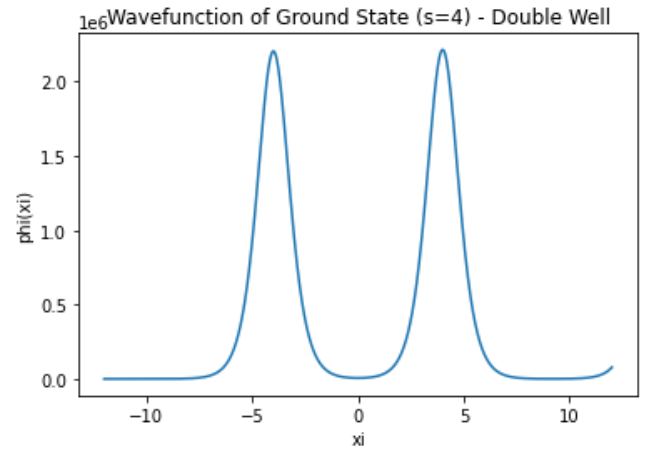


FIG. 7: The figure shows the plot for the wave function of the ground state for the double well potential model with the x-axis being the value of  $\xi$  while the y-axis is  $\phi(\xi)$ . The graph displays the results of running the code in the Appendix in Section VI, which is based on equation (7).

3.3) The two energies we found for large  $s$  values were close to the energies found in the single well analysis. The two energies are  $-3.99935$  and  $-1.00296$  which are similar to the values provided in Figures 4 and 5 respectively. They do appear to be “almost degenerate” as seen in Figures 7 and 8, appearing like two isolated systems.

3.4) The wave functions for the double well potential have similar features to the single well potential that hint at linear combinations. as they are pair-wise similar as seen by the figures.

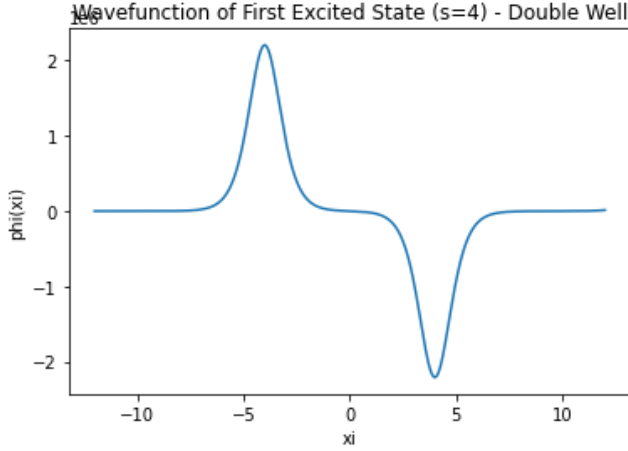


FIG. 8: The figure shows the plot for the wave function of the first excited state for the double well potential model with the x-axis being the value of  $\xi$  while the y-axis is  $\phi(\xi)$ . The graph displays the results of running the code in the Appendix in Section VI, which is based on equation (7).

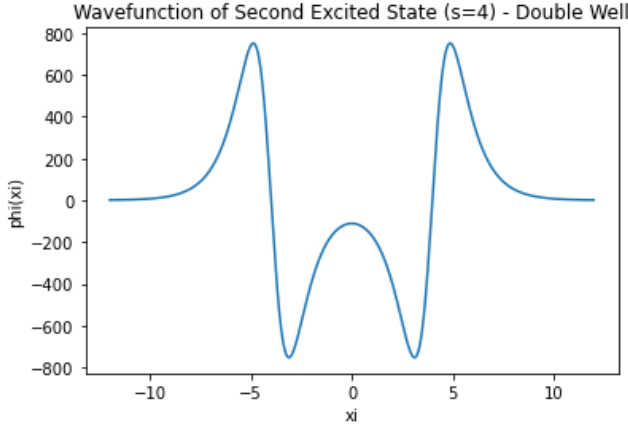


FIG. 9: The figure shows the plot for the wave function of the second excited state for the double well potential model with the x-axis being the value of  $\xi$  while the y-axis is  $\phi(\xi)$ . The graph displays the results of running the code in the Appendix in Section VI, which is based on equation (7).

Figure 7 looks like a combination of two Figure 4 graphs centered around  $\xi = 0$ , Figure 8 looks similar to Figure 5, and Figure 9 looks like a linear combination of two Figure 5 graphs centered around  $\xi = 0$ .

## V. DISCUSSION

The study involved the implementation of numerical methods to solve the Schrödinger equation, specifically using the shooting method, bisection method, and double-well potential models. The shooting method was employed to determine the number of nodes for the

ground state and first excited state wave functions, yielding results presented in Figures 2 and 3. The ground state wave function was found to have zero nodes, while the first excited state wave function had one node. Additionally, the excited state extended further into space due to its higher energy eigenvalue, allowing the wave function to penetrate deeper into regions of lower potential energy.

The bisection method was utilized to calculate the energy eigenvalues for the ground state and first excited state systems. The results, shown in Figures 4 and 5, indicated that an upper energy limit of  $\epsilon = 1$  was recommended to prevent inaccuracies when the energy value approximates zero. However, due to time constraints, further exploration of large initial values ( $\nu_0$ ) and associated eigenenergies was not conducted.

The analysis was extended to double-well potential models using similar computational techniques. The relationship between the separation parameter ( $s$ ) and energy eigenvalues was examined, as shown in Figure 6. For small values of  $s$ , three bound states were observed, while for large values of  $s$ , two bound states were found. The obtained energy values for small  $s$  were somewhat similar to those from the single well potential, while energies for large  $s$  approached those of the single well analysis.

The wave functions for the ground state, first excited state, and second excited state in the double well potential were visualized in Figures 7, 8, and 9, respectively. Notably, these wave functions exhibited similarities to their counterparts in the single well potential, suggesting linear combinations.

Overall, the numerical methods employed in this study provided insights into the wave functions and energy eigenvalues of different potential models, offering a valuable approach to solving the Schrödinger equation.

## VI. APPENDIX

### Shooting Method

```
# -*- coding: utf-8 -*-
"""
Created on Tue May 16 08:29:26 2023

@author: Alex Matilainen
"""

import numpy as np
import matplotlib.pyplot as plt
# Parameters
ximax=8
ximin=-ximax
Nsteps=100*2*ximax
h=(2*ximax)/Nsteps
nu0=6.0

xi=np.linspace(-ximax,ximax,Nsteps)
phi=np.zeros(Nsteps)

nu=-nu0*(np.cosh(xi))**(-2)
```

```
eps= -3.9990186 #-3.9990186 (ground), -.998 (excited)
```

```
elif (val > 0):
    eps_max = eps
```

```
q=np.sqrt(-eps)
phi[0]=1
phi[1]=np.exp(q*h)
```

```
print(eps)
```

```
for i in range(2,Nsteps):
    phi[i]=(2+h**2*(nu[i-1]-eps))*phi[i-1]-phi[i-2]
```

```
plt.plot(xi,phi)
plt.xlabel("xi")
plt.ylabel("phi(xi)")
plt.title("Title")
plt.show()
```

```
plt.plot(xi,phi)
plt.xlabel("xi")
plt.ylabel("phi(xi)")
plt.title("Title")
plt.show()
```

## Double-Well Potential Model

### Bisection Method

```
# -*- coding: utf-8 -*-
"""
```

```
Created on Tue May 16 09:40:36 2023
```

```
@author: Alex Matilainen
"""
```

```
import numpy as np
import matplotlib.pyplot as plt
# Parameters
ximax=8
ximin=-ximax
Nsteps=100*2*ximax
h=(2*ximax)/Nsteps
nu0=6.0
```

```
xi=np.linspace(-ximax,ximax,Nsteps)
# phi_min=np.zeros(Nsteps)
# phi_max=np.zeros(Nsteps)
```

```
nu=-nu0*(np.cosh(xi))**(-2)
eps_min=-nu0
eps_max=-0.1
q_min=np.sqrt(-eps_min)
q_max=np.sqrt(-eps_max)
phi=np.zeros(Nsteps)
```

```
state = 1 # 0 for ground state, 1 for first excited state
```

```
while ((np.abs(eps_min-eps_max)/np.abs(eps_min+eps_max)) > 10**-8):
```

```
    eps = (eps_min + eps_max) / 2
    q=np.sqrt(-eps)
    phi[0]=1
    phi[1]=np.exp(q*h)
```

```
    nodes = 0
```

```
    for i in range(2,Nsteps):
        phi[i]=(2+h**2*(nu[i-1]-eps))*phi[i-1]-phi[i-2]
        if (phi[i]*phi[i-1] < 0):
            nodes += 1
```

```
    if (nodes < state):
        eps_min = eps
    elif (nodes > state):
        eps_max = eps
```

```
    else:
        val = phi[Nsteps-1]*phi[Nsteps-2]-np.exp(q*h)*(phi[Nsteps-1]-phi[Nsteps-2])
        if (val < 0):
            # [Nsteps-1]**2
            eps_min=eps
```

```
# -*- coding: utf-8 -*-
"""
```

```
Created on Wed May 17 08:03:01 2023
```

```
@author: Alex Matilainen
"""
```

```
import numpy as np
import matplotlib.pyplot as plt
# Parameters
for state in range(0,3):
    rec = 40
    stot = np.linspace(0.1,4,rec)
    epsvals = np.zeros(rec)
    index = 0
```

```
for s in stot:
    ximax=int(s+8)
    ximin=-ximax
    Nsteps=100*2*ximax
    h=(2*ximax)/Nsteps
    nu0=6.0
```

```
xi=np.linspace(-ximax,ximax,Nsteps)
```

```
nu1=-nu0*(np.cosh(xi+s))**(-2)
nu2=-nu0*(np.cosh(xi-s))**(-2)
nu=nu1+nu2
eps_min=-2*nu0
eps_max=-0.1
q_min=np.sqrt(-eps_min)
q_max=np.sqrt(-eps_max)
```

```
phi=np.zeros(Nsteps) #phi=np.zeros(Nsteps)
```

```
while ((np.abs(eps_min-eps_max)/np.abs(eps_min+eps_max)) > 10**-8):
    # -max)) > 10**-8):
```

```
    eps = (eps_min + eps_max) / 2
    q=np.sqrt(-eps)
    phi[0]=1
    phi[1]=np.exp(q*h)
```

```
    nodes = 0
```

```
for i in range(2,Nsteps):
    phi[i]=(2+h**2*(nu[i-1]-eps))*phi[i-1]-phi[i-2]
    if (phi[i]*phi[i-1] < 0):
        nodes += 1
```

```
if (nodes < state):
    eps_min = eps
elif (nodes > state):
    eps_max = eps
```

```

else:
    val = phi[Nsteps-1]*phi[Nsteps-2]-np.exp(q*h)*(phi[Nsteps-1])**2
    if (val < 0):
        eps_min=eps
    elif (val > 0):
        eps_max = eps
        plt.plot(stot, epsvals, '. ')

epsvals[index] = eps
index += 1

plt.legend(["ground_state", "first_state", "second_state"])
plt.title("Title")
plt.xlabel("Separation_Value_(s)")
plt.ylabel("Eigenenergy_value_(eps)")
# if s==4: ## Used for finding ground
# state and excited state for large s (s=4) # plt.xlim(0,4) ## Wavefunctions of high s
# plt.plot(xi, phi)
# plt.xlabel("xi")
# plt.ylabel("phi(xi)")
# if state == 0: #ground
#     plt.title("Title")
# elif state == 1: #first excited
#     plt.title("Title")
# plt.show()

plt.xlim(-0.1*10**(9), 3.3*10**(9))
plt.show()

```

## VII. ACKNOWLEDGMENTS

All three group members set up and performed the experiment. Natalie wrote the introduction and theoretical background; Alex wrote the results and appendix; Iman wrote the methods and discussion.

---

[1] Lab Manual Computer Lab  
<https://canvas.education.lu.se/courses/22074/>